

First direct measurement of the absolute branching fraction of $\Sigma^+ \rightarrow \Lambda e^+ \nu_e$

M. Ablikim,¹ M. N. Achasov,^{13,b} P. Adlarson,⁷³ R. Aliberti,³⁴ A. Amoroso,^{72a,72c} M. R. An,³⁸ Q. An,^{69,56} Y. Bai,⁵⁵ O. Bakina,³⁵ R. Baldini Ferroli,^{28a} I. Balossino,^{29a} Y. Ban,^{45,g} V. Batozskaya,^{1,43} D. Becker,³⁴ K. Begzsuren,³¹ N. Berger,³⁴ M. Bertani,^{28a} D. Bettoni,^{29a} F. Bianchi,^{72a,72c} E. Bianco,^{72a,72c} J. Bloms,⁶⁶ A. Bortone,^{72a,72c} I. Boyko,³⁵ R. A. Briere,⁵ A. Brueggemann,⁶⁶ H. Cai,⁷⁴ X. Cai,^{1,56} A. Calcaterra,^{28a} G. F. Cao,^{1,61} N. Cao,^{1,61} S. A. Cetin,^{60a} J. F. Chang,^{1,56} T. T. Chang,⁷⁵ W. L. Chang,^{1,61} G. R. Che,⁴² G. Chelkov,^{35,a} C. Chen,⁴² Chao Chen,⁵³ G. Chen,¹ H. S. Chen,^{1,61} M. L. Chen,^{1,56,61} S. J. Chen,⁴¹ S. M. Chen,⁵⁹ T. Chen,^{1,61} X. R. Chen,^{30,61} X. T. Chen,^{1,61} Y. B. Chen,^{1,56} Y. Q. Chen,³³ Z. J. Chen,^{25,h} W. S. Cheng,^{72c} S. Choi,¹⁰ S. K. Choi,⁵³ X. Chu,⁴² G. Cibinetto,^{29a} S. C. Coen,⁴ F. Cossio,^{72c} J. J. Cui,⁴⁸ H. L. Dai,^{1,56} J. P. Dai,⁷⁷ A. Dbeysi,¹⁹ R. E. de Boer,⁴ D. Dedovich,³⁵ Z. Y. Deng,¹ A. Denig,³⁴ I. Denysenko,³⁵ M. Destefanis,^{72a,72c} F. De Mori,^{72a,72c} Y. Ding,³⁹ Y. Ding,³³ J. Dong,^{1,56} L. Y. Dong,^{1,61} M. Y. Dong,^{1,56,61} X. Dong,⁷⁴ S. X. Du,⁷⁹ Z. H. Duan,⁴¹ P. Egorov,^{35,a} Y. L. Fan,⁷⁴ J. Fang,^{1,56} S. S. Fang,^{1,61} W. X. Fang,¹ Y. Fang,¹ R. Farinelli,^{29a} L. Fava,^{72b,72c} F. Feldbauer,⁴ G. Felici,^{28a} C. Q. Feng,^{69,56} J. H. Feng,⁵⁷ K. Fischer,⁶⁷ M. Fritsch,⁴ C. Fritsch,⁶⁶ C. D. Fu,¹ Y. W. Fu,¹ H. Gao,⁶¹ Y. N. Gao,^{45,g} Yang Gao,^{69,56} S. Garbolino,^{72c} I. Garzia,^{29a,29b} P. T. Ge,⁷⁴ Z. W. Ge,⁴¹ C. Geng,⁵⁷ E. M. Gersabeck,⁶⁵ A. Gilman,⁶⁷ K. Goetzen,¹⁴ L. Gong,³⁹ W. X. Gong,^{1,56} W. Gradl,³⁴ M. Greco,^{72a,72c} M. H. Gu,^{1,56} Y. T. Gu,¹⁶ C. Y. Guan,^{1,61} Z. L. Guan,²² A. Q. Guo,^{30,61} L. B. Guo,⁴⁰ R. P. Guo,⁴⁷ Y. P. Guo,^{12,f} A. Guskov,^{35,a} W. Y. Han,³⁸ X. Q. Hao,²⁰ F. A. Harris,⁶³ K. K. He,⁵³ K. L. He,^{1,61} F. H. Heinsius,⁴ C. H. Heinz,³⁴ Y. K. Heng,^{1,56,61} C. Herold,⁵⁸ T. Holtmann,⁴ P. C. Hong,^{12,f} G. Y. Hou,^{1,61} X. T. Hou,^{1,61} Y. R. Hou,⁶¹ Z. L. Hou,¹ H. M. Hu,^{1,61} J. F. Hu,^{54,i} T. Hu,^{1,56,61} Y. Hu,¹ G. S. Huang,^{69,56} K. X. Huang,⁵⁷ L. Q. Huang,^{30,61} X. T. Huang,⁴⁸ Y. P. Huang,¹ T. Hussain,⁷¹ N. Hüsken,^{27,34} W. Imoehl,²⁷ M. Irshad,^{69,56} J. Jackson,²⁷ S. Jaeger,⁴ S. Janchiv,³¹ E. Jang,⁵³ J. H. Jeong,⁵³ Q. Ji,¹ Q. P. Ji,²⁰ X. B. Ji,^{1,61} X. L. Ji,^{1,56} Y. Y. Ji,⁴⁸ Z. K. Jia,^{69,56} P. C. Jiang,^{45,g} S. S. Jiang,³⁸ T. J. Jiang,¹⁷ X. S. Jiang,^{1,56,61} Y. Jiang,⁶¹ J. B. Jiao,⁴⁸ Z. Jiao,²³ S. Jin,⁴¹ Y. Jin,⁶⁴ M. Q. Jing,^{1,61} T. Johansson,⁷³ S. Kabana,³² N. Kalantar-Nayestanaki,⁶² X. L. Kang,⁹ X. S. Kang,³⁹ R. Kappert,⁶² M. Kavatsyuk,⁶² B. C. Ke,⁷⁹ A. Khoukaz,⁶⁶ R. Kiuchi,¹ R. Kliemt,¹⁴ L. Koch,³⁶ O. B. Kolcu,^{60a} B. Kopf,⁴ M. Kuessner,⁴ X. Kui,¹ A. Kupsc,^{43,73} W. Kühn,³⁶ J. J. Lane,⁶⁵ J. S. Lange,³⁶ P. Larin,¹⁹ A. Lavanaia,²⁶ L. Lavezzi,^{72a,72c} T. T. Lei,^{69,k} Z. H. Lei,^{69,56} H. Leithoff,³⁴ M. Lellmann,³⁴ T. Lenz,³⁴ C. Li,⁴² C. Li,⁴⁶ C. H. Li,³⁸ Cheng Li,^{69,56} D. M. Li,⁷⁹ F. Li,^{1,56} G. Li,¹ H. Li,^{69,56} H. B. Li,^{1,61} H. J. Li,²⁰ H. N. Li,^{54,i} Hui Li,⁴² J. R. Li,⁵⁹ J. S. Li,⁵⁷ J. W. Li,⁴⁸ Ke Li,¹ L. J. Li,^{1,61} L. K. Li,¹ Lei Li,³ M. H. Li,⁴² P. R. Li,^{37,j,k} S. X. Li,¹² S. Y. Li,⁵⁹ T. Li,⁴⁸ W. D. Li,^{1,61} W. G. Li,¹ X. H. Li,^{69,56} X. L. Li,⁴⁸ Xiaoyu Li,^{1,61} Y. G. Li,^{45,g} Z. J. Li,⁵⁷ Z. X. Li,¹⁶ Z. Y. Li,⁵⁷ C. Liang,⁴¹ H. Liang,^{69,56} H. Liang,³³ H. Liang,^{1,61} Y. F. Liang,⁵² Y. T. Liang,^{30,61} G. R. Liao,¹⁵ L. Z. Liao,⁴⁸ J. Libby,²⁶ A. Limphirat,⁵⁸ D. X. Lin,^{30,61} T. Lin,¹ B. X. Liu,⁷⁴ B. J. Liu,¹ C. Liu,³³ C. X. Liu,¹ D. Liu,^{19,69} F. H. Liu,⁵¹ Fang Liu,¹ Feng Liu,⁶ G. M. Liu,^{54,i} H. Liu,^{37,j,k} H. B. Liu,¹⁶ H. M. Liu,^{1,61} Huanhuan Liu,¹ Huihui Liu,²¹ J. B. Liu,^{69,56} J. L. Liu,⁷⁰ J. Y. Liu,^{1,61} K. Liu,¹ K. Y. Liu,³⁹ Ke Liu,²² L. Liu,^{69,56} L. C. Liu,⁴² Lu Liu,⁴² M. H. Liu,^{12,f} P. L. Liu,¹ Q. Liu,⁶¹ S. B. Liu,^{69,56} T. Liu,^{12,f} W. K. Liu,⁴² W. M. Liu,^{69,56} X. Liu,^{37,j,k} Y. Liu,^{37,j,k} Y. B. Liu,⁴² Z. A. Liu,^{1,56,61} Z. Q. Liu,⁴⁸ X. C. Lou,^{1,56,61} F. X. Lu,⁵⁷ H. J. Lu,²³ J. G. Lu,^{1,56} X. L. Lu,¹ Y. Lu,⁷ Y. P. Lu,^{1,56} Z. H. Lu,^{1,61} C. L. Luo,⁴⁰ M. X. Luo,⁷⁸ T. Luo,^{12,f} X. L. Luo,^{1,56} X. R. Lyu,⁶¹ Y. F. Lyu,⁴² F. C. Ma,³⁹ H. L. Ma,¹ J. L. Ma,^{1,61} L. L. Ma,⁴⁸ M. M. Ma,^{1,61} Q. M. Ma,¹ R. Q. Ma,^{1,61} R. T. Ma,⁶¹ X. Y. Ma,^{1,56} Y. Ma,^{45,g} F. E. Maas,¹⁹ M. Maggiora,^{72a,72c} S. Maldaner,⁴ S. Malde,⁶⁷ A. Mangoni,^{28b} Y. J. Mao,^{45,g} Z. P. Mao,¹ S. Marcello,^{72a,72c} Z. X. Meng,⁶⁴ J. G. Messchendorp,^{14,62} G. Mezzadri,^{29a} H. Miao,^{1,61} T. J. Min,⁴¹ R. E. Mitchell,²⁷ X. H. Mo,^{1,56,61} N. Yu. Muchnoi,^{13,b} Y. Nefedov,³⁵ F. Nerling,^{19,d} I. B. Nikolaev,^{13,b} Z. Ning,^{1,56} S. Nisar,^{11,1} Y. Niu,⁴⁸ S. L. Olsen,⁶¹ Q. Ouyang,^{1,56,61} S. Pacetti,^{28b,28c} X. Pan,⁵³ Y. Pan,⁵⁵ A. Pathak,³³ Y. P. Pei,^{69,56} M. Pelizaeus,⁴ H. P. Peng,^{69,56} K. Peters,^{14,d} J. L. Ping,⁴⁰ R. G. Ping,^{1,61} S. Plura,³⁴ S. Pogodin,³⁵ V. Prasad,^{69,56} F. Z. Qi,¹ H. Qi,^{69,56} H. R. Qi,⁵⁹ M. Qi,⁴¹ T. Y. Qi,^{12,f} S. Qian,^{1,56} W. B. Qian,⁶¹ C. F. Qiao,⁶¹ J. J. Qin,⁷⁰ L. Q. Qin,¹⁵ X. P. Qin,^{12,f} X. S. Qin,⁴⁸ Z. H. Qin,^{1,56} J. F. Qiu,¹ S. Q. Qu,⁵⁹ C. F. Redmer,³⁴ K. J. Ren,³⁸ A. Rivetti,^{72c} V. Rodin,⁶² M. Rolo,^{72c} G. Rong,^{1,61} Ch. Rosner,¹⁹ S. N. Ruan,⁴² A. Sarantsev,^{35,c} Y. Schelhaas,³⁴ K. Schoenning,⁷³ M. Scodreggio,^{29a,29b} K. Y. Shan,^{12,f} W. Shan,²⁴ X. Y. Shan,^{69,56} J. F. Shangguan,⁵³ L. G. Shao,^{1,61} M. Shao,^{69,56} C. P. Shen,^{12,f} H. F. Shen,^{1,61} W. H. Shen,⁶¹ X. Y. Shen,^{1,61} B. A. Shi,⁶¹ H. C. Shi,^{69,56} J. Y. Shi,¹ Q. Q. Shi,⁵³ R. S. Shi,^{1,61} X. Shi,^{1,56} J. J. Song,²⁰ T. Z. Song,⁵⁷ W. M. Song,^{33,1} Y. X. Song,^{45,g} S. Sosio,^{72a,72c} S. Spataro,^{72a,72c} F. Stielor,³⁴ Y. J. Su,⁶¹ G. B. Sun,⁷⁴ G. X. Sun,¹ H. Sun,⁶¹ H. K. Sun,¹ J. F. Sun,²⁰ K. Sun,⁵⁹ L. Sun,⁷⁴ S. S. Sun,^{1,61} T. Sun,^{1,61} W. Y. Sun,³³ Y. Sun,⁹ Y. J. Sun,^{69,56} Y. Z. Sun,¹ Z. T. Sun,⁴⁸ Y. X. Tan,^{69,56} C. J. Tang,⁵² G. Y. Tang,¹ J. Tang,⁵⁷ Y. A. Tang,⁷⁴ L. Y. Tao,⁷⁰ Q. T. Tao,^{25,h} M. Tat,⁶⁷ J. X. Teng,^{69,56} V. Thoren,⁷³ W. H. Tian,⁵⁰ W. H. Tian,⁵⁷ Y. Tian,^{30,61} Z. F. Tian,⁷⁴ I. Uman,^{60b} B. Wang,¹ B. Wang,^{69,56} B. L. Wang,⁶¹ C. W. Wang,⁴¹ D. Y. Wang,^{45,g} F. Wang,⁷⁰ H. J. Wang,^{37,j,k} H. P. Wang,^{1,61} K. Wang,^{1,56} L. L. Wang,¹ M. Wang,⁴⁸ Meng Wang,^{1,61} S. Wang,^{12,f}

T. Wang,^{12,f} T. J. Wang,⁴² W. Wang,⁷⁰ W. Wang,⁵⁷ W. H. Wang,⁷⁴ W. P. Wang,^{69,56} X. Wang,^{45,g} X. F. Wang,^{37,j,k}
 X. J. Wang,³⁸ X. L. Wang,^{12,f} Y. Wang,⁵⁹ Y. D. Wang,⁴⁴ Y. F. Wang,^{1,56,61} Y. H. Wang,⁴⁶ Y. N. Wang,⁴⁴ Y. Q. Wang,¹
 Yaqian Wang,^{18,1} Yi Wang,⁵⁹ Z. Wang,^{1,56} Z. L. Wang,⁷⁰ Z. Y. Wang,^{1,61} Ziyi Wang,⁶¹ D. Wei,⁶⁸ D. H. Wei,¹⁵
 F. Weidner,⁶⁶ S. P. Wen,¹ C. W. Wenzel,⁴ U. Wiedner,⁴ G. Wilkinson,⁶⁷ M. Wolke,⁷³ L. Wollenberg,⁴ C. Wu,³⁸
 J. F. Wu,^{1,61} L. H. Wu,¹ L. J. Wu,^{1,61} X. Wu,^{12,f} X. H. Wu,³³ Y. Wu,⁶⁹ Y. J. Wu,³⁰ Z. Wu,^{1,56} L. Xia,^{69,56} X. M. Xian,³⁸
 T. Xiang,^{45,g} D. Xiao,^{37,j,k} G. Y. Xiao,⁴¹ H. Xiao,^{12,f} S. Y. Xiao,¹ Y. L. Xiao,^{12,f} Z. J. Xiao,⁴⁰ C. Xie,⁴¹ X. H. Xie,^{45,g}
 Y. Xie,⁴⁸ Y. G. Xie,^{1,56} Y. H. Xie,⁶ Z. P. Xie,^{69,56} T. Y. Xing,^{1,61} C. F. Xu,^{1,61} C. J. Xu,⁵⁷ G. F. Xu,¹ H. Y. Xu,⁶⁴ Q. J. Xu,¹⁷
 X. P. Xu,⁵³ Y. C. Xu,⁷⁶ Z. P. Xu,⁴¹ F. Yan,^{12,f} L. Yan,^{12,f} W. B. Yan,^{69,56} W. C. Yan,⁷⁹ X. Q. Yan,¹ H. J. Yang,^{49,e}
 H. L. Yang,³³ H. X. Yang,¹ Tao Yang,¹ Y. Yang,^{12,f} Y. F. Yang,⁴² Y. X. Yang,^{1,61} Yifan Yang,^{1,61} M. Ye,^{1,56} M. H. Ye,⁸
 J. H. Yin,¹ Z. Y. You,⁵⁷ B. X. Yu,^{1,56,61} C. X. Yu,⁴² G. Yu,^{1,61} T. Yu,⁷⁰ X. D. Yu,^{45,g} C. Z. Yuan,^{1,61} L. Yuan,²
 S. C. Yuan,¹ X. Q. Yuan,¹ Y. Yuan,^{1,61} Z. Y. Yuan,⁵⁷ C. X. Yue,³⁸ A. A. Zafar,⁷¹ F. R. Zeng,⁴⁸ X. Zeng,^{12,f} Y. Zeng,^{25,h}
 X. Y. Zhai,³³ Y. H. Zhan,⁵⁷ A. Q. Zhang,^{1,61} B. L. Zhang,^{1,61} B. X. Zhang,¹ D. H. Zhang,⁴² G. Y. Zhang,²⁰
 H. Zhang,⁶⁹ H. H. Zhang,³³ H. H. Zhang,⁵⁷ H. Q. Zhang,^{1,56,61} H. Y. Zhang,^{1,56} J. J. Zhang,⁵⁰ J. L. Zhang,⁷⁵
 J. Q. Zhang,⁴⁰ J. W. Zhang,^{1,56,61} J. X. Zhang,^{37,j,k} J. Y. Zhang,¹ J. Z. Zhang,^{1,61} Jianyu Zhang,^{1,61}
 Jiawei Zhang,^{1,61} L. M. Zhang,⁵⁹ L. Q. Zhang,⁵⁷ Lei Zhang,⁴¹ P. Zhang,¹ Q. Y. Zhang,^{38,79} Shuihan Zhang,^{1,61}
 Shulei Zhang,^{25,h} X. D. Zhang,⁴⁴ X. M. Zhang,¹ X. Y. Zhang,⁴⁸ X. Y. Zhang,⁵³ Y. Zhang,⁶⁷ Y. T. Zhang,⁷⁹ Y. H. Zhang,^{1,56}
 Yan Zhang,^{69,56} Yao Zhang,¹ Z. H. Zhang,¹ Z. L. Zhang,³³ Z. Y. Zhang,⁷⁴ Z. Y. Zhang,⁴² G. Zhao,¹ J. Zhao,³⁸
 J. Y. Zhao,^{1,61} J. Z. Zhao,^{1,56} Lei Zhao,^{69,56} Ling Zhao,¹ M. G. Zhao,⁴² S. J. Zhao,⁷⁹ Y. B. Zhao,^{1,56} Y. X. Zhao,^{30,61}
 Z. G. Zhao,^{69,56} A. Zhemchugov,^{35,a} B. Zheng,⁷⁰ J. P. Zheng,^{1,56} W. J. Zheng,^{1,61} Y. H. Zheng,⁶¹ B. Zhong,⁴⁰
 X. Zhong,⁵⁷ H. Zhou,⁴⁸ L. P. Zhou,^{1,61} X. Zhou,⁷⁴ X. K. Zhou,⁶¹ X. R. Zhou,^{69,56} X. Y. Zhou,³⁸ Y. Z. Zhou,^{12,f} J. Zhu,⁴²
 K. Zhu,¹ K. J. Zhu,^{1,56,61} L. Zhu,³³ L. X. Zhu,⁶¹ S. H. Zhu,⁶⁸ S. Q. Zhu,⁴¹ T. J. Zhu,^{12,f} W. J. Zhu,^{12,f} Y. C. Zhu,^{69,56}
 Z. A. Zhu,^{1,61} J. H. Zou,¹ and J. Zu^{69,56}

(BESIII Collaboration)

¹*Institute of High Energy Physics, Beijing 100049, People's Republic of China*

²*Beihang University, Beijing 100191, People's Republic of China*

³*Beijing Institute of Petrochemical Technology, Beijing 102617, People's Republic of China*

⁴*Bochum Ruhr-University, D-44780 Bochum, Germany*

⁵*Carnegie Mellon University, Pittsburgh, Pennsylvania 15213, USA*

⁶*Central China Normal University, Wuhan 430079, People's Republic of China*

⁷*Central South University, Changsha 410083, People's Republic of China*

⁸*China Center of Advanced Science and Technology, Beijing 100190, People's Republic of China*

⁹*China University of Geosciences, Wuhan 430074, People's Republic of China*

¹⁰*Chung-Ang University, Republic of Korea*

¹¹*COMSATS University Islamabad, Lahore Campus, Defence Road, Off Raiwind Road, 54000 Lahore, Pakistan*

¹²*Fudan University, Shanghai 200433, People's Republic of China*

¹³*G.I. Budker Institute of Nuclear Physics SB RAS (BINP), Novosibirsk 630090, Russia*

¹⁴*GSI Helmholtzcentre for Heavy Ion Research GmbH, D-64291 Darmstadt, Germany*

¹⁵*Guangxi Normal University, Guilin 541004, People's Republic of China*

¹⁶*Guangxi University, Nanning 530004, People's Republic of China*

¹⁷*Hangzhou Normal University, Hangzhou 310036, People's Republic of China*

¹⁸*Hebei University, Baoding 071002, People's Republic of China*

¹⁹*Helmholtz Institute Mainz, Staudinger Weg 18, D-55099 Mainz, Germany*

²⁰*Henan Normal University, Xinxiang 453007, People's Republic of China*

²¹*Henan University of Science and Technology, Luoyang 471003, People's Republic of China*

²²*Henan University of Technology, Zhengzhou 450001, People's Republic of China*

²³*Huangshan College, Huangshan 245000, People's Republic of China*

²⁴*Hunan Normal University, Changsha 410081, People's Republic of China*

²⁵*Hunan University, Changsha 410082, People's Republic of China*

- ²⁶*Indian Institute of Technology Madras, Chennai 600036, India*
- ²⁷*Indiana University, Bloomington, Indiana 47405, USA*
- ^{28a}*INFN Laboratori Nazionali di Frascati, I-00044, Frascati, Italy*
- ^{28b}*INFN Sezione di Perugia, I-06100, Perugia, Italy*
- ^{28c}*University of Perugia, I-06100, Perugia, Italy*
- ^{29a}*INFN Sezione di Ferrara, I-44122, Ferrara, Italy*
- ^{29b}*University of Ferrara, I-44122, Ferrara, Italy*
- ³⁰*Institute of Modern Physics, Lanzhou 730000, People's Republic of China*
- ³¹*Institute of Physics and Technology, Peace Avenue 54B,
Ulaanbaatar 13330, Mongolia*
- ³²*Instituto de Alta Investigación, Universidad de Tarapacá, Casilla 7D, Arica, Chile*
- ³³*Jilin University, Changchun 130012, People's Republic of China*
- ³⁴*Johannes Gutenberg University of Mainz, Johann-Joachim-Becher-Weg 45,
D-55099 Mainz, Germany*
- ³⁵*Joint Institute for Nuclear Research, 141980 Dubna, Moscow region, Russia*
- ³⁶*Justus-Liebig-Universität Giessen, II. Physikalisches Institut, Heinrich-Buff-Ring 16,
D-35392 Giessen, Germany*
- ³⁷*Lanzhou University, Lanzhou 730000, People's Republic of China*
- ³⁸*Liaoning Normal University, Dalian 116029, People's Republic of China*
- ³⁹*Liaoning University, Shenyang 110036, People's Republic of China*
- ⁴⁰*Nanjing Normal University, Nanjing 210023, People's Republic of China*
- ⁴¹*Nanjing University, Nanjing 210093, People's Republic of China*
- ⁴²*Nankai University, Tianjin 300071, People's Republic of China*
- ⁴³*National Centre for Nuclear Research, Warsaw 02-093, Poland*
- ⁴⁴*North China Electric Power University, Beijing 102206, People's Republic of China*
- ⁴⁵*Peking University, Beijing 100871, People's Republic of China*
- ⁴⁶*Qufu Normal University, Qufu 273165, People's Republic of China*
- ⁴⁷*Shandong Normal University, Jinan 250014, People's Republic of China*
- ⁴⁸*Shandong University, Jinan 250100, People's Republic of China*
- ⁴⁹*Shanghai Jiao Tong University, Shanghai 200240, People's Republic of China*
- ⁵⁰*Shanxi Normal University, Linfen 041004, People's Republic of China*
- ⁵¹*Shanxi University, Taiyuan 030006, People's Republic of China*
- ⁵²*Sichuan University, Chengdu 610064, People's Republic of China*
- ⁵³*Soochow University, Suzhou 215006, People's Republic of China*
- ⁵⁴*South China Normal University, Guangzhou 510006, People's Republic of China*
- ⁵⁵*Southeast University, Nanjing 211100, People's Republic of China*
- ⁵⁶*State Key Laboratory of Particle Detection and Electronics,
Beijing 100049, Hefei 230026, People's Republic of China*
- ⁵⁷*Sun Yat-Sen University, Guangzhou 510275, People's Republic of China*
- ⁵⁸*Suranaree University of Technology, University Avenue 111, Nakhon Ratchasima 30000, Thailand*
- ⁵⁹*Tsinghua University, Beijing 100084, People's Republic of China*
- ^{60a}*Istinye University, 34010, Istanbul, Turkey*
- ^{60b}*Near East University, Nicosia, North Cyprus, 99138, Mersin 10, Turkey*
- ⁶¹*University of Chinese Academy of Sciences, Beijing 100049, People's Republic of China*
- ⁶²*University of Groningen, NL-9747 AA Groningen, Netherlands*
- ⁶³*University of Hawaii, Honolulu, Hawaii 96822, USA*
- ⁶⁴*University of Jinan, Jinan 250022, People's Republic of China*
- ⁶⁵*University of Manchester, Oxford Road, Manchester, M13 9PL, United Kingdom*
- ⁶⁶*University of Muenster, Wilhelm-Klemm-Strasse 9, 48149 Muenster, Germany*
- ⁶⁷*University of Oxford, Keble Road, Oxford OX13RH, United Kingdom*
- ⁶⁸*University of Science and Technology Liaoning, Anshan 114051,
People's Republic of China*
- ⁶⁹*University of Science and Technology of China, Hefei 230026,
People's Republic of China*
- ⁷⁰*University of South China, Hengyang 421001, People's Republic of China*
- ⁷¹*University of the Punjab, Lahore-54590, Pakistan*
- ^{72a}*University of Turin, I-10125, Turin, Italy*
- ^{72b}*University of Eastern Piedmont, I-15121, Alessandria, Italy*
- ^{72c}*INFN, I-10125, Turin, Italy*
- ⁷³*Uppsala University, Box 516, SE-75120 Uppsala, Sweden*

⁷⁴Wuhan University, Wuhan 430072, People's Republic of China
⁷⁵Xinyang Normal University, Xinyang 464000, People's Republic of China
⁷⁶Yantai University, Yantai 264005, People's Republic of China
⁷⁷Yunnan University, Kunming 650500, People's Republic of China
⁷⁸Zhejiang University, Hangzhou 310027, People's Republic of China
⁷⁹Zhengzhou University, Zhengzhou 450001, People's Republic of China

 (Received 12 December 2022; accepted 30 March 2023; published 28 April 2023)

The first direct measurement of the absolute branching fraction of $\Sigma^+ \rightarrow \Lambda e^+ \nu_e$ is reported based on an e^+e^- annihilation sample of $(10087 \pm 44) \times 10^6$ J/ψ events collected with the BESIII detector at $\sqrt{s} = 3.097$ GeV. The branching fraction is determined to be $\mathcal{B}(\Sigma^+ \rightarrow \Lambda e^+ \nu_e) = [2.93 \pm 0.74(\text{stat}) \pm 0.13(\text{syst})] \times 10^{-5}$, which is the most precise measurement obtained in a single experiment to date and also the first result obtained at a collider experiment. Combining this result with the world average of $\mathcal{B}(\Sigma^- \rightarrow \Lambda e^- \bar{\nu}_e)$ and the lifetimes of Σ^\pm , the ratio, $\frac{\Gamma(\Sigma^- \rightarrow \Lambda e^- \bar{\nu}_e)}{\Gamma(\Sigma^+ \rightarrow \Lambda e^+ \nu_e)}$, is determined to be 1.06 ± 0.28 , which is within 1.8 standard deviations of the value expected in the absence of second-class currents.

DOI: 10.1103/PhysRevD.107.072010

Weinberg first remarked that the weak hadronic currents of spin-parity (J^P) can be classified as two types according to their transformation properties under G parity [1]. The first-class currents have the vector currents with $G = +1$ and the axial currents with $G = -1$, and are expected to be

dominant. Whereas the second-class currents own the opposite G parities, and are suppressed since they are connected with the mass difference of light up and down quarks. They will vanish in the limit of $m_u = m_d$ (i.e. isospin symmetry); thus they are allowed to appear in the Standard Model. However, there is not any experimental evidence been found for the second-class currents up to date.

^aAlso at the Moscow Institute of Physics and Technology, Moscow 141700, Russia.

^bAlso at the Novosibirsk State University, Novosibirsk, 630090, Russia.

^cAlso at the NRC “Kurchatov Institute,” PNPI, 188300, Gatchina, Russia.

^dAlso at Goethe University Frankfurt, 60323 Frankfurt am Main, Germany.

^eAlso at Key Laboratory for Particle Physics, Astrophysics and Cosmology, Ministry of Education; Shanghai Key Laboratory for Particle Physics and Cosmology; Institute of Nuclear and Particle Physics, Shanghai 200240, People's Republic of China.

^fAlso at Key Laboratory of Nuclear Physics and Ion-beam Application (MOE) and Institute of Modern Physics, Fudan University, Shanghai 200443, People's Republic of China.

^gAlso at State Key Laboratory of Nuclear Physics and Technology, Peking University, Beijing 100871, People's Republic of China.

^hAlso at School of Physics and Electronics, Hunan University, Changsha 410082, China.

ⁱAlso at Guangdong Provincial Key Laboratory of Nuclear Science, Institute of Quantum Matter, South China Normal University, Guangzhou 510006, China.

^jAlso at Frontiers Science Center for Rare Isotopes, Lanzhou University, Lanzhou 730000, People's Republic of China.

^kAlso at Lanzhou Center for Theoretical Physics, Lanzhou University, Lanzhou 730000, People's Republic of China.

^lAlso at the Department of Mathematical Sciences, IBA, Karachi, Pakistan.

The decay $\tau^- \rightarrow \eta \pi^- \nu_\tau$ is forbidden in the absence of second-class currents, which was once claimed to have been evidenced with an unexpectedly large branching fraction $(5.1 \pm 1.5)\%$ [2]. However, this branching fraction is measured afterward to be less than 7.3×10^{-5} and 9.9×10^{-5} by Belle [3] and BABAR [4], respectively. Previous nuclear β decay experiments gave contradictory conclusions concerning the existence of second-class currents. Positive signals have been reported by F.P. Calaprice *et al.* [5], in which the result requires a second-class form factor comparable to the weak-magnetism term, and by K. Sugimoto *et al.* [6–8], where the experimental results are in favor of the existence of the second-class induced-tensor current. On the other hand, D. H. Wilkinson *et al.* [9–12] reported the absence of second-class currents. In addition, studies on hyperon semileptonic weak decays have been performed, where the existence of second-class currents will yield a nonzero pseudotensor term (g_2) in the matrix element of the axial-vector current [13], and some of the polarized Λ experiments suggest a large g_2 [14]. Such a nonzero g_2 value could be caused by flavor-SU(3)-symmetry-breaking effects [15,16], or it could reflect the existence of a new interaction in the weak Hamiltonian involving second-class currents. To distinguish between genuine second-class currents and flavor-SU(3)-symmetry-breaking effects, a unique observable was first proposed by S. Weinberg [1] in 1958,

$$R \equiv \frac{\Gamma(\Sigma^- \rightarrow \Lambda e^- \bar{\nu}_e)}{\Gamma(\Sigma^+ \rightarrow \Lambda e^+ \nu_e)} = \frac{\mathcal{B}(\Sigma^- \rightarrow \Lambda e^- \bar{\nu}_e) \times \tau_{\Sigma^+}}{\mathcal{B}(\Sigma^+ \rightarrow \Lambda e^+ \nu_e) \times \tau_{\Sigma^-}}, \quad (1)$$

where $\Gamma(\Sigma^- \rightarrow \Lambda e^- \bar{\nu}_e)$ and $\Gamma(\Sigma^+ \rightarrow \Lambda e^+ \nu_e)$ are the partial widths of the decay channels $\Sigma^- \rightarrow \Lambda e^- \bar{\nu}_e$ and $\Sigma^+ \rightarrow \Lambda e^+ \nu_e$, respectively; $\mathcal{B}(\Sigma^- \rightarrow \Lambda e^- \bar{\nu}_e)$ and $\mathcal{B}(\Sigma^+ \rightarrow \Lambda e^+ \nu_e)$ are the branching fractions of the above two channels; τ_{Σ^-} and τ_{Σ^+} are the life times of Σ^- and Σ^+ , respectively. In the absence of second-class currents, this R value should be just the phase-space ratio for these two decays whether flavor-SU(3)-symmetry-breaking effects exist or not, so any experimental deviation from this expectation would be decisive evidence for the existence of second-class currents [1]. In 1960, the theoretical prediction of this R value was calculated to be 1.57 by T. D. Lee and C. N. Yang [17] on the basis of no second-class currents.

In the late 1960s, the decay $\Sigma^\pm \rightarrow \Lambda e^\pm \nu$ was studied at fixed-target experiments [18–20]. All the experimentally determined R values are consistent with the theoretical calculation, i.e. 1.57, within uncertainty. In the following years, the precisions of τ_{Σ^\pm} and $\mathcal{B}(\Sigma^- \rightarrow \Lambda e^- \bar{\nu}_e)$ measurements have been improved significantly, but the current experimental uncertainty of R [21] is still large due to the poor precision of $\mathcal{B}(\Sigma^+ \rightarrow \Lambda e^+ \nu_e)$. Previously, there were three experimental results of $\mathcal{B}(\Sigma^+ \rightarrow \Lambda e^+ \nu_e)$, and all of them are indirect measurements [22] from fixed-target experiments, which were performed more than 50 years ago [18–20]. The highest precision measurement of $\mathcal{B}(\Sigma^+ \rightarrow \Lambda e^+ \nu_e)$ was performed in 1969 based on 10 signal events [19], which were selected from about 6×10^6 bubble chamber pictures. Therefore, a direct measurement of $\mathcal{B}(\Sigma^+ \rightarrow \Lambda e^+ \nu_e)$ at a modern collider experiment with higher precision is crucial to provide a more stringent test of the existence of second-class currents.

In this article, we report the first direct measurement of the absolute branching fraction $\mathcal{B}(\Sigma^+ \rightarrow \Lambda e^+ \nu_e)$, by analyzing $\Sigma^+ \bar{\Sigma}^-$ hyperon pairs in $(10087 \pm 44) \times 10^6$ [23] J/ψ events collected with the BESIII detector at $\sqrt{s} = 3.097$ GeV. The J/ψ meson decays into the $\Sigma^+ \bar{\Sigma}^-$ final state with a branching fraction of $(1.07 \pm 0.04) \times 10^{-3}$ [21]. We use the double-tag (DT) technique [24], which provides a clean and direct branching fraction measurement without requiring knowledge of the total number of $\Sigma^+ \bar{\Sigma}^-$ events produced. Based on the measured absolute branching fraction of $\Sigma^+ \rightarrow \Lambda e^+ \nu_e$, a higher precision R is determined. Throughout this paper, the charge-conjugated (*c.c.*) channel is always implied.

Details about the design and performance of the BESIII detector are given in Ref. [25]. Simulated data samples produced with Geant4-based [26] Monte Carlo (MC) software, which includes the geometric description of the BESIII detector [27] and the detector response, are used to determine the detection efficiencies and to estimate backgrounds. The simulation includes the beam energy

spread and initial state radiation in the e^+e^- annihilations modeled with the generator KKMC [28]. For the simulation of the signal channel $\Sigma^+ \rightarrow \Lambda e^+ \nu_e$, we use the model reported in Ref. [29], which has been validated in Ref. [30], and use the form factors obtained from the SU(3) flavor parametrization and the Cabibbo theory, which are summarized in Ref. [13]. The inclusive MC sample of generic events includes both the production of the J/ψ resonance and the continuum processes incorporated in KKMC [28]. All particle decays are modeled with EvtGen [31] using branching fractions either taken from the Particle Data Group (PDG), when available, or estimated with LUNDCHARM [32] for J/ψ resonance. Final state radiation from charged final state particles is incorporated using PHOTOS [33].

Using the DT technique, the branching fraction is obtained by reconstructing signal $\Sigma^+ \rightarrow \Lambda e^+ \nu_e$ decay in events with $\bar{\Sigma}^-$ decays reconstructed in their dominant hadronic decay mode $\bar{\Sigma}^- \rightarrow \bar{p}\pi^0$, where the Λ and π^0 decays are reconstructed through $\Lambda \rightarrow p\pi^-$ and $\pi^0 \rightarrow \gamma\gamma$, respectively. If a $\bar{\Sigma}^-$ hyperon is found, then it is referred to as a single-tag (ST) candidate. An event in which a signal Σ^+ decay and a ST $\bar{\Sigma}^-$ are simultaneously found is referred to as a DT event. The branching fraction of the signal decay is given by

$$\mathcal{B}_{\text{sig}} = \frac{N_{\text{DT}}/\epsilon_{\text{DT}}}{N_{\text{ST}}/\epsilon_{\text{ST}}} \times \frac{1}{\mathcal{B}(\Lambda \rightarrow p\pi^-)}, \quad (2)$$

where N_{DT} is the DT yield, ϵ_{DT} is the DT efficiency, $\mathcal{B}(\Lambda \rightarrow p\pi^-)$ is the branching fraction of $\Lambda \rightarrow p\pi^-$, and N_{ST} and ϵ_{ST} are the ST yield and the ST efficiency, respectively.

Charged tracks detected in the main drift chamber (MDC) are required to be within a polar angle (θ) range of $|\cos\theta| < 0.93$, where θ is defined with respect to the z axis, which is the symmetry axis of the MDC. Photon candidates are identified using showers in the electromagnetic calorimeter (EMC). The deposited energy of each shower must be more than 25 MeV in the barrel region ($|\cos\theta| < 0.80$) and more than 50 MeV in the end cap region ($0.86 < |\cos\theta| < 0.92$). To exclude showers that originate from charged tracks, the angle subtended by the EMC shower and the position of the closest charged track at the EMC must be greater than 10 degrees as measured from the interaction point. To suppress electronic noise and showers unrelated to the event, the difference between the EMC time and the event start time is required to be within [0, 700] ns.

Particle identification (PID) for charged tracks combines measurements of the specific ionization energy loss in the MDC (dE/dx) and the flight time in the time-of-flight system to form likelihoods $\mathcal{L}(h)$ ($h = p, K, \pi$) for various hadron h hypotheses. A track is identified as a proton when the proton hypothesis has the greatest likelihood [$\mathcal{L}(p) > \mathcal{L}(K)$ and $\mathcal{L}(p) > \mathcal{L}(\pi)$] and satisfies $\mathcal{L}(p) > 0.001$. The π^0 candidates are reconstructed by

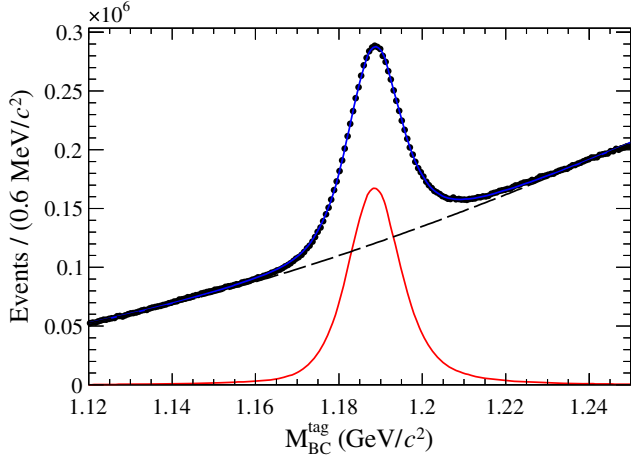


FIG. 1. Fit to the $M_{\text{BC}}^{\text{tag}}$ distribution of the ST $\bar{\Sigma}^- + \text{c.c.}$ candidates. Data are shown as dots with error bars. The solid blue, solid red, and dashed black curves are the fit result, signal shape, and the background shape, respectively.

performing a one constraint (1C) kinematic fit on the chosen photon pair, constraining the invariant mass of the photon pair to the nominal π^0 mass, and the $\chi^2_{1\text{C}}$ of the kinematic fit is required to be less than 25. Events with at least one antiproton and one π^0 are assigned as ST $\bar{\Sigma}^-$ candidates.

Next, tagged $\bar{\Sigma}^-$ hyperons are selected using two kinematic variables, the energy difference

$$\Delta E_{\text{tag}} \equiv E_{\text{beam}} - E_{\bar{\Sigma}^-}, \quad (3)$$

and the beam-constrained mass

$$M_{\text{BC}}^{\text{tag}} c^2 \equiv \sqrt{E_{\text{beam}}^2 - |\vec{p}_{\bar{\Sigma}^-} c|^2}, \quad (4)$$

where E_{beam} is the beam energy, $\vec{p}_{\bar{\Sigma}^-}$ and $E_{\bar{\Sigma}^-}$ are the momentum and the energy of the $\bar{\Sigma}^-$ candidate in the e^+e^- rest frame, respectively. If there are multiple combinations, the one giving the minimum $|\Delta E_{\text{tag}}|$ is retained for further analysis. The tagged $\bar{\Sigma}^-$ candidates are required to satisfy $\Delta E_{\text{tag}} \in [-48, 52]$ MeV.

The yield of ST $\bar{\Sigma}^-$ hyperons is obtained from a binned extended maximum likelihood fit to the $M_{\text{BC}}^{\text{tag}}$ distribution of the surviving ST candidates, where the signal is modeled by the MC-simulated signal shape convolved with a Gaussian function to account for imperfect simulation of the detector resolution, and the background is modeled by a third-order Chebyshev function. The fit result is shown in Fig. 1, and the total ST $\bar{\Sigma}^-$ yield is $N_{\text{ST}} = 4, 693, 360 \pm 4, 339(\text{stat})$.

Candidate events for the $\Sigma^+ \rightarrow \Lambda e^+ \nu_e$, $\Lambda \rightarrow p \pi^-$ decays are selected from the remaining tracks recoiling against the ST $\bar{\Sigma}^-$ events in the mass region $|M_{\text{BC}}^{\text{tag}} - m_{\bar{\Sigma}^-}| < 0.049$ GeV/ c^2 , where $m_{\bar{\Sigma}^-}$ is the $\bar{\Sigma}^-$

nominal mass. The total number of charged tracks in the event is required to be four ($N_{\text{Track}} = 4$), and the selection criteria for the additional charged tracks are the same as those used in the ST selection. We further identify a charged track as an e^+ by requiring the PID likelihoods, including also the EMC information, satisfy $\mathcal{L}'(e)/(\mathcal{L}'(e) + \mathcal{L}'(\pi) + \mathcal{L}'(K)) > 0.8$, where $\mathcal{L}'(e)$, $\mathcal{L}'(\pi)$, $\mathcal{L}'(K)$ are likelihoods calculated based on the positron, pion, and kaon hypotheses, respectively. A π^- candidate is required to satisfy $\mathcal{L}'(\pi) > \mathcal{L}'(K)$ and $\mathcal{L}'(\pi) > \mathcal{L}'(e)$. The other track is assumed to be a proton. Each Λ candidate is reconstructed from a proton and a pion, which are constrained to originate from a common vertex and are required to fall in an invariant mass region $|M_{p\pi^-} - m_{\Lambda}| < 10$ MeV/ c^2 , where m_{Λ} is the Λ nominal mass [21]. The decay length of the Λ candidate from the interaction point is required to be greater than twice the vertex resolution.

As the neutrino is not detected, we employ the kinematic variable

$$M_{\text{miss}}^2 c^4 \equiv E_{\text{miss}}^2 - p_{\text{miss}}^2 c^2, \quad (5)$$

where E_{miss} and p_{miss} are the missing energy and momentum carried by the neutrino, respectively. E_{miss} is calculated by

$$E_{\text{miss}} = E_{\text{beam}} - E_{\Lambda} - E_{e^+}, \quad (6)$$

where E_{Λ} and E_{e^+} are the energies of the Λ and e^+ calculated in the e^+e^- rest frame, respectively. To obtain better resolution, we use the constrained Σ^+ momentum (\vec{p}_{Σ^+}) given by

$$\vec{p}_{\Sigma^+} = -\frac{\vec{p}_{\bar{\Sigma}^-}}{c|\vec{p}_{\bar{\Sigma}^-}|} \sqrt{E_{\text{beam}}^2 - m_{\Sigma^+}^2 c^4}, \quad (7)$$

to calculate p_{miss}

$$p_{\text{miss}} = |\vec{p}_{\Sigma^+} - \vec{p}_{\Lambda} - \vec{p}_{e^+}|, \quad (8)$$

where \vec{p}_{Λ} and \vec{p}_{e^+} are the momenta of Λ and e^+ calculated in the e^+e^- rest frame, respectively. For signal events, M_{miss}^2 is expected to peak at zero.

For the signal candidates of $\Sigma^+ \rightarrow \Lambda e^+ \nu_e$ decay, there are still some non- $\Sigma^+ \bar{\Sigma}^-$ pair background events. Therefore, we require that the opening angle between the antiproton and π^0 in $\bar{\Sigma}^-$ rest frame satisfies $\text{Angle}(\bar{p}, \pi^0) > 170^\circ$, and the momentum of the antiproton in the $\bar{\Sigma}^-$ rest frame satisfies $p_{\bar{p}}^{\text{ST}} \in [0.16, 0.21]$ GeV/ c , where the $\bar{\Sigma}^-$ rest frame is determined by making use of the fact that $J/\psi \rightarrow \Sigma^+ \bar{\Sigma}^-$ is a two-body reaction. To further suppress backgrounds, we impose two extra requirements as follows. First, the $\bar{\Sigma}^- \Lambda$ recoil mass calculated using $M_{\bar{\Sigma}^- \Lambda}^{\text{recoil}} + M_{p\pi^-} - m_{\Lambda}$ is

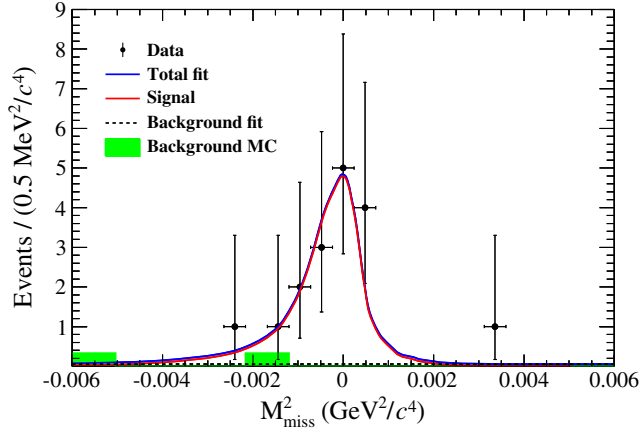


FIG. 2. Fit to the M_{miss}^2 distribution of the DT candidates. Data are shown as dots with error bars. The solid blue and red curves are the fit result and signal shape, respectively. The black dashed curve is the background shape. The green-filled histogram is the background estimated from the inclusive MC sample.

required to be greater than $-60 \text{ MeV}/c^2$, which can suppress the contributions from Σ^+ hadronic decay and other combinatorial background. $M_{\Sigma^-\Lambda}^{\text{recoil}}$ is formed by

$$M_{\Sigma^-\Lambda}^{\text{recoil}} c^2 = \sqrt{(E_{\Sigma^-\Lambda}^{\text{recoil}})^2 - (p_{\Sigma^-\Lambda}^{\text{recoil}})^2 c^2}, \quad (9)$$

where $E_{\Sigma^-\Lambda}^{\text{recoil}}$ and $p_{\Sigma^-\Lambda}^{\text{recoil}}$ are the total energy and the total momentum of all recoiling particles against $\Sigma^-\Lambda$ in an event, which are calculated by

$$E_{\Sigma^-\Lambda}^{\text{recoil}} = E_{\text{beam}} - E_{\Lambda}, \quad (10)$$

and

$$p_{\Sigma^-\Lambda}^{\text{recoil}} = |\vec{p}_{\Sigma^+} - \vec{p}_{\Lambda}| \quad (11)$$

respectively (E_{Λ} , \vec{p}_{Σ^+} , and \vec{p}_{Λ} are calculated in the e^+e^- rest frame). The variable $M_{\Sigma^-\Lambda}^{\text{recoil}} + M_{p\pi^-} - m_{\Lambda}$ can provide improved resolution compared to $M_{\Sigma^-\Lambda}^{\text{recoil}}$ [34,35]. Second, the decay of $\Sigma(1385)^+ \rightarrow \Lambda\pi^+$ could contribute as background when the pion is wrongly identified as a positron. If we assign the π^+ mass to the e^+ candidates when calculating the invariant mass of Λe^+ , i.e. $M_{\Lambda(\pi^+ \rightarrow e^+)}$, the $\Sigma(1385)^+$ mass is expected for the background. Therefore, we can eliminate background by only retaining the events with $M_{\Lambda(\pi^+ \rightarrow e^+)} < 1.32 \text{ GeV}/c^2$. The above four requirements can effectively suppress the backgrounds, with a signal efficiency loss of less than 1% for each requirement.

The inclusive MC sample is analyzed using the `TopoAna` [36] package to study potential backgrounds. After imposing the above selection criteria, the contribution from the $\Sigma^+\Sigma^-$ pair background is negligible, and there are only a few non- $\Sigma^+\Sigma^-$ pair background events surviving, which are shown as the green filled histogram in Fig. 2.

To determine the signal yield, an unbinned extended maximum likelihood fit is performed to the M_{miss}^2 distribution. The signal is modeled by the MC-simulated signal shape convolved with a Gaussian resolution function. The background is modeled by a flat background shape. The parameters of the Gaussian and all yields are free in the fit. The fit to the data is shown in Fig. 2, and N_{ST} , ϵ_{ST} , N_{DT} , and ϵ_{DT} are summarized in Table I.

The systematic uncertainty due to the requirement for $N_{\text{Track}} = 4$ (2.7%) is studied with the control sample of ($J/\psi \rightarrow \Lambda\bar{\Lambda}$, $\Lambda \rightarrow p\pi^-$, $\bar{\Lambda} \rightarrow \bar{p}\pi^+$) [30], while the uncertainty for Λ reconstruction (1.1%) is studied with the control samples of ($J/\psi \rightarrow \bar{p}K^+\Lambda$, $\Lambda \rightarrow p\pi^- + \text{c.c.}$) and $J/\psi \rightarrow p\bar{p}\pi^+\pi^-$ [37]. The uncertainties due to the tracking (1.0%) and PID (2.3%) for the positron are studied with the control sample $e^+e^- \rightarrow \gamma e^+e^-$ [38]. For the simulation of the signal MC model (0.6%), it is estimated by varying the input values of form factors [13] by one standard deviation. The uncertainties due to the fits to the M_{miss}^2 (0.3%) and $M_{\text{BC}}^{\text{tag}}$ (1.8%) distributions are estimated by using alternative fit procedures, i.e. changing the signal and background shapes for both of these fits and changing the bin size for the fit to the $M_{\text{BC}}^{\text{tag}}$ distribution. For the branching fraction $\mathcal{B}(\Lambda \rightarrow p\pi^-)$, the uncertainty is 0.8% [21]. The total systematic uncertainty is estimated to be 4.4% by adding all these uncertainties in quadrature.

Finally, by using N_{ST} , ϵ_{ST} , N_{DT} , and ϵ_{DT} summarized in Table I and the well-measured $\mathcal{B}(\Lambda \rightarrow p\pi^-) = (63.9 \pm 0.5)\%$ from the PDG into Eq. (2), the corresponding branching fraction is determined to be $\mathcal{B}(\Sigma^+ \rightarrow \Lambda e^+\nu_e) = (2.93 \pm 0.74 \pm 0.13) \times 10^{-5}$, where the first uncertainty is statistical and the second is systematic. Combining with the well-measured branching fraction of $\Sigma^- \rightarrow \Lambda e^-\bar{\nu}_e$ [$\mathcal{B}(\Sigma^- \rightarrow \Lambda e^-\bar{\nu}_e) = (5.73 \pm 0.27) \times 10^{-5}$] and the lifetimes of Σ^\pm [$\tau_{\Sigma^-} = (1.479 \pm 0.011) \times 10^{-10} \text{ s}$ and $\tau_{\Sigma^+} = (8.018 \pm 0.026) \times 10^{-11} \text{ s}$] [21], we determine the R value defined in Eq. (1) to be $R = 1.06 \pm 0.28$. This result is within 1.8 standard deviations of the theoretical calculation [17] in the absence of second-class currents.

In summary, using $(10087 \pm 44) \times 10^6$ J/ψ decay events collected with the BESIII detector at $\sqrt{s} = 3.097 \text{ GeV}$, the semileptonic hyperon decay $\Sigma^+ \rightarrow \Lambda e^+\nu_e$ is studied at a collider experiment for the first time. This is also the first experimental study after a more than 50-year hiatus. Based on the DT method, we perform the first direct measurement of the absolute branching fraction of $\Sigma^+ \rightarrow \Lambda e^+\nu_e$ to be $\mathcal{B}(\Sigma^+ \rightarrow \Lambda e^+\nu_e) = [2.93 \pm 0.74(\text{stat}) \pm 0.13(\text{syst})] \times 10^{-5}$,

TABLE I. Values of N_{ST} , N_{DT} , ϵ_{ST} , and ϵ_{DT} used for the branching fraction determination. The uncertainties are statistical only.

N_{ST}	N_{DT}	$\epsilon_{\text{ST}} (\%)$	$\epsilon_{\text{DT}} (\%)$
$4,693,360 \pm 4,339$	15.7 ± 4.0	41.48 ± 0.03	7.40 ± 0.01

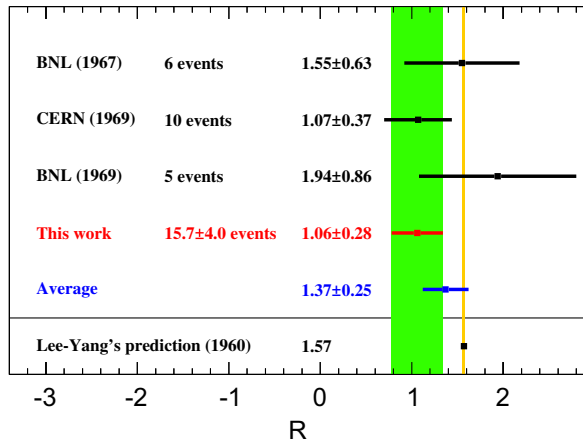


FIG. 3. R value obtained in this work, compared to the recalculated values by previous fixed-target experiments [BNL (1967) [20], CERN (1969) [19], BNL (1969) [18]], the updated weighted average and the Lee-Yang's prediction (1960) on the basis of no second-class currents [17].

which is consistent with all the previous indirect measurements within uncertainty and is the most precise result (about 25% improvement in precision) obtained in a single experiment to date [21]. Combining with the well-measured branching fraction of $\Sigma^- \rightarrow \Lambda e^- \bar{\nu}_e$ and the lifetimes of Σ^\pm , we determine the R value defined in Eq. (1) to be $R = 1.06 \pm 0.28$. Figure 3 shows the comparison between our R value and the prediction of Ref. [17], together with values from previous fixed-target experiments [18–20] recalculated with the latest PDG values of $\mathcal{B}(\Sigma^- \rightarrow \Lambda e^- \bar{\nu}_e)$ and τ_{Σ^\pm} ; we present the updated weighted average R value, including our measurement, as 1.37 ± 0.25 . This paper contributes to the most precise measurement of R in a single experiment; this result is within 1.8 standard deviations of the theoretical calculation [17] in the absence of second-class currents.

The BESIII collaboration thanks the staff of BEPCII and the IHEP computing center for their strong support. The authors thank Prof. Ru-Min Wang for helpful discussions. This work is supported in part by National Key R&D Program of China under Contracts No. 2020YFA0406300,

No. 2020YFA0406400; National Natural Science Foundation of China (NSFC) under Contracts No. 11805037, No. 11635010, No. 11735014, No. 11835012, No. 11935015, No. 11935016, No. 11935018, No. 11961141012, No. 12022510, No. 12025502, No. 12035009, No. 12035013, No. 12061131003, No. 12192260, No. 12192261, No. 12192262, No. 12192263, No. 12192264, No. 12192265; No. 12165022; the Chinese Academy of Sciences (CAS) Large-Scale Scientific Facility Program; the CAS Center for Excellence in Particle Physics (CCEPP); Joint Large-Scale Scientific Facility Funds of the NSFC and CAS under Contract No. U1832121, No. U1832207; CAS Key Research Program of Frontier Sciences under Contracts No. QYZDJ-SSW-SLH003, No. QYZDJ-SSW-SLH040; 100 Talents Program of CAS; The Institute of Nuclear and Particle Physics (INPAC) and Shanghai Key Laboratory for Particle Physics and Cosmology; Yunnan Fundamental Research Project under Contract No. 202301AT070162; ERC under Contract No. 758462; European Union's Horizon 2020 research and innovation programme under Marie Skłodowska-Curie Grant Agreement No. 894790; German Research Foundation DFG under Contracts No. 443159800, No. 455635585, Collaborative Research Center CRC 1044, FOR5327, GRK 2149; Istituto Nazionale di Fisica Nucleare, Italy; Ministry of Development of Turkey under Contract No. DPT2006K-120470; National Science and Technology fund; National Science Research and Innovation Fund (NSRF) via the Program Management Unit for Human Resources & Institutional Development, Research and Innovation under Contract No. B16F640076; Olle Engkvist Foundation under Contract No. 200-0605; Polish National Science Centre under Contract No. 2019/35/O/ST2/02907; STFC (United Kingdom); Suranaree University of Technology (SUT), Thailand Science Research and Innovation (TSRI), and National Science Research and Innovation Fund (NSRF) under Contract No. 160355; The Royal Society, UK under Contracts No. DH140054, No. DH160214; The Swedish Research Council; U.S. Department of Energy under Contract No. DE-FG02-05ER41374.

- [1] S. Weinberg, *Phys. Rev.* **112**, 1375 (1958).
- [2] M. Derrick *et al.*, *Phys. Lett. B* **189**, 260 (1987).
- [3] K. Hayasaka (Belle Collaboration), *Proc. Sci. EPS-HEP2009* (2009) 374.
- [4] P. del Amo Sanchez *et al.* (BABAR Collaboration), *Phys. Rev. D* **83**, 032002 (2011).
- [5] F. P. Calaprice, S. J. Freedman, W. C. Mead, and H. C. Vantine, *Phys. Rev. Lett.* **35**, 1566 (1975).

- [6] K. Sugimoto, I. Tanihata, and J. Göring, *Phys. Rev. Lett.* **34**, 1533 (1975).
- [7] C. J. Bowers, S. J. Freedman, B. Fujikawa, A. O. Macchiavelli, R. W. MacLeod, J. Reich, S. Q. Shang, P. A. Vetter, and E. Wasserman, *Phys. Rev. C* **59**, 1113 (1999).
- [8] S. Triambak *et al.*, *Phys. Rev. C* **95**, 035501 (2017).
- [9] D. H. Wilkinson and D. E. Alburger, *Phys. Rev. Lett.* **26**, 1127 (1971).

- [10] R. E. Tribble and G. T. Garvey, *Phys. Rev. Lett.* **32**, 314 (1974); *Phys. Rev. C* **12**, 967 (1975).
- [11] D. Wilkinson, *Eur. Phys. J. A* **7**, 307 (2000).
- [12] K. Minamisono *et al.*, *Phys. Rev. C* **84**, 055501 (2011).
- [13] N. Cabibbo, E. C. Swallow, and R. Winston, *Annu. Rev. Nucl. Part. Sci.* **53**, 39 (2003).
- [14] Augusto Garcia, *Phys. Rev. D* **3**, 2638 (1971).
- [15] P. L. Pritchett and N. G. Deshpande, *Phys. Rev. D* **8**, 2963 (1973).
- [16] S. Sasaki and T. Yamazaki, *Phys. Rev. D* **79**, 074508 (2009).
- [17] T. D. Lee and C. N. Yang, *Phys. Rev.* **119**, 1410 (1960).
- [18] C. Baltay, P. Franzini, R. Newman, H. Norton, N. Yeh, J. Cole, J. Lee-Franzini, R. Loveless, and J. McFadyen, *Phys. Rev. Lett.* **22**, 615 (1969).
- [19] F. Eisele *et al.*, *Z. Phys.* **221**, 1 (1969).
- [20] N. Barash, T. B. Day, R. G. Glasser, B. Kehoe, R. Knop, B. Sechi-Zorn, and G. A. Snow, *Phys. Rev. Lett.* **19**, 181 (1967).
- [21] R. L. Workman *et al.* (Particle Data Group), *Prog. Theor. Exp. Phys.* **2022**, 083C01 (2022).
- [22] In the previous measurements of $\mathcal{B}(\Sigma^+ \rightarrow \Lambda e^+ \nu_e)$ [18–20], in order to get the branching fraction, they had to determine the total number of produced Σ^+ at first. In Refs. [18,19], they deduced the number of produced Σ^+ using the production rate of $\frac{\Sigma^+}{\Sigma^-}$. In Ref. [20], they determined the number of produced Σ^+ by counting the number of Σ^+ s decaying into protons.
- [23] M. Ablikim *et al.* (BESIII Collaboration), *Chin. Phys. C* **46**, 074001 (2022).
- [24] R. M. Baltrusaitis *et al.* (MARK III Collaboration), *Phys. Rev. Lett.* **56**, 2140 (1986); J. Adler *et al.* (MARK III Collaboration), *Phys. Rev. Lett.* **60**, 89 (1988).
- [25] M. Ablikim *et al.* (BESIII Collaboration), *Nucl. Instrum. Methods Phys. Res., Sect. A* **614**, 345 (2010).
- [26] S. Agostinelli *et al.* (Geant4 Collaboration), *Nucl. Instrum. Methods Phys. Res., Sect. A* **506**, 250 (2003).
- [27] K. X. Huang, Z. J. Li, Z. Qian, J. Zhu, H. Y. Li, Y. M. Zhang, S. S. Sun, and Z. Y. You, *Nuclear Science and Techniques* **33**, 142 (2022).
- [28] S. Jadach, B. F. L. Ward, and Z. Was, *Phys. Rev. D* **63**, 113009 (2001); *Comput. Phys. Commun.* **130**, 260 (2000).
- [29] R. M. Wang, M. Z. Yang, H. B. Li, and X. D. Cheng, *Phys. Rev. D* **100**, 076008 (2019).
- [30] M. Ablikim *et al.* (BESIII Collaboration), *Phys. Rev. Lett.* **127**, 121802 (2021).
- [31] D. J. Lange, *Nucl. Instrum. Methods Phys. Res., Sect. A* **462**, 152 (2001); R. G. Ping, *Chin. Phys. C* **32**, 599 (2008).
- [32] J. C. Chen, G. S. Huang, X. R. Qi, D. H. Zhang, and Y. S. Zhu, *Phys. Rev. D* **62**, 034003 (2000); R. L. Yang, R. G. Ping, and H. Chen, *Chin. Phys. Lett.* **31**, 061301 (2014).
- [33] E. Richter-Was, *Phys. Lett. B* **303**, 163 (1993).
- [34] M. Ablikim *et al.* (BESIII Collaboration), *Phys. Rev. Lett.* **112**, 132001 (2014).
- [35] M. Ablikim *et al.* (BESIII Collaboration), *Phys. Rev. Lett.* **126**, 102001 (2021).
- [36] X. Y. Zhou, S. X. Du, G. Li, and C. P. Shen, *Comput. Phys. Commun.* **258**, 107540 (2021).
- [37] M. Ablikim *et al.* (BESIII Collaboration), *Phys. Rev. Lett.* **121**, 062003 (2018).
- [38] M. Ablikim *et al.* (BESIII Collaboration), *Phys. Rev. D* **103**, 052011 (2021).